

Fast calculation of carrier harmonic iron losses caused by pulse width modulation in interior permanent magnet synchronous motors

Zhu, Sa; Dong, Jianning; Li, Yanru; Hua, Wei

DOI

[10.1049/iet-epa.2019.0837](https://doi.org/10.1049/iet-epa.2019.0837)

Publication date

2020

Document Version

Accepted author manuscript

Published in

IET Electric Power Applications

Citation (APA)

Zhu, S., Dong, J., Li, Y., & Hua, W. (2020). Fast calculation of carrier harmonic iron losses caused by pulse width modulation in interior permanent magnet synchronous motors. *IET Electric Power Applications*, 14(7), 1163-1176. <https://doi.org/10.1049/iet-epa.2019.0837>

Important note

To cite this publication, please use the final published version (if applicable). Please check the document version above.

Copyright

Other than for strictly personal use, it is not permitted to download, forward or distribute the text or part of it, without the consent of the author(s) and/or copyright holder(s), unless the work is under an open content license such as Creative Commons.

Takedown policy

Please contact us and provide details if you believe this document breaches copyrights. We will remove access to the work immediately and investigate your claim.

Rotor Stress Analysis of High-Speed Permanent Magnet Machines with Segmented Magnets Retained by Carbon-Fibre Sleeve

Journal:	<i>IEEE Transactions on Energy Conversion</i>
Manuscript ID	TEC-00226-2020.R1
Manuscript Type:	Transactions
Date Submitted by the Author:	10-Jul-2020
Complete List of Authors:	Wang, Yu; The University of Sheffield, EEE Zhu, Z.Q.; University of Sheffield, Dept. of Electronic and Electrical Engineering Feng, Jianghua; CRRC Corp., Zhuzhou Guo, Shuying; CRRC Corp., Zhuzhou Li, Y. F.; CRRC Corp., Zhuzhou Wang, Yu; CRRC Corp., Zhuzhou
Technical Topic Area:	Electrical machinery theory < Electric Machinery
Key Words:	Permanent magnet machines, Brushless rotating machines, Permanent magnets, Rotating machine mechanical factors

Rotor Stress Analysis of High-Speed Permanent Magnet Machines with Segmented Magnets Retained by Carbon-Fibre Sleeve

Y. Wang, Z.Q. Zhu, *Fellow, IEEE*, J.H. Feng, S.Y. Guo, Y. F. Li, and Y. Wang

Abstract—In this paper, the rotor stress is analysed for a high-speed permanent magnet (PM) machine (HSPMM) with segmented magnets retained by a carbon-fibre sleeve. The influence of rotor PM segmentation is firstly considered in the stress analysis. It is found that when the segmented magnets are under tensile stress, significant sleeve stress concentration will occur due to magnet edging effect. By contrast, the PMs will benefit from the segmentation with reduced tangential stress. This stress reduction effect is enhanced when the number of PM segments is larger. Furthermore, the influence of PM segmentation on the worst operating scenario is determined. In order to avoid stress concentration due to PM segmentation, the design guidelines are then given by investigating the influence of sleeve thickness and interference fit. A new design scheme of sleeve thickness is proposed based on the identified worst case scenarios. Finally, a 6-slot 4-pole high speed PM machine with segmented magnets retained by carbon-fibre sleeve is prototyped and tested at the speed of 90krpm. The rotor stability indirectly indicates the validity of the theoretical analysis and design scheme.

Index Terms—carbon-fibre sleeve, high-speed machines, permanent magnet, rotor stress, segmentation.

I. INTRODUCTION

High-speed PM machines (HSPMMs) are very promising for high-speed applications due to higher efficiency, power factor, and utilization factor in comparison with other types of high-speed electrical machines. However, there are still many obstacles and challenges for the HSPMM design, especially on the rotor side. Significant rotor eddy-current loss and rotor mechanical stress will be produced under high-speed operation. Fig.1 illustrates typical rotor cross-section of a high-speed PM machine. Normally, the rotor pole numbers of high-speed PM machines are selected to be 2 or 4, depending on specific requirements and constraints. The 2-pole rotor structure is preferred in the low-power ultra-high-speed applications due to a lower fundamental frequency which is easier for control and also beneficial to the reduction of stator iron loss and rotor PM eddy-current loss [1]-[4]. On the other hand, the 4-pole rotor is more inclined to be adopted for high-power high-speed applications due to reduced end-winding length and stator copper loss, which are quite advantageous for stator thermal equilibrium in high power application [5]-[8]. However, the relatively high fundamental frequency introduced by higher pole number will inevitably lead to higher rotor PM eddy-current loss. Hence, for the 4-pole high-speed PM machine, the rotor magnets are usually segmented to reduce the PM eddy-current loss.

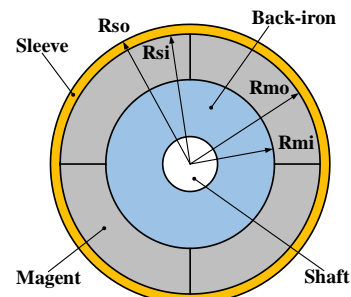


Fig.1. Cross-section of a typical 4-pole high-speed PM machine rotor.

In addition, as shown in Fig.1, the rotor magnets are retained by the sleeve to withstand the extremely high mechanical stress resulting from high speed. Generally, the retaining sleeves can be classified into two types: Non-metallic ones and metallic ones. Glass-fibre and carbon-fibre are typical non-metallic sleeves which are featured with high yield strength and low mass density [6]. This is quite desirable for the protection of PMs. In addition, the sleeve thickness can be maintained minimum for a given operating speed so that its influence on the amplitude of air gap flux density can be minimized. The main issue for this type of sleeve is the thermal aspect. The thermal conductivity of carbon-fibre material is quite low which means the heat generated from the rotor magnets cannot be dissipated easily [9]. Hence, the rotor magnets are normally segmented to reduce the eddy-current loss. Alternatively, the copper shield can be placed at the inner side of carbon-fibre sleeve [10]. On the other hand, the metallic sleeves made of titanium or Inconel are equipped with a relatively lower strength to density ratio compared to that of carbon-fibre. The advantages of metallic sleeve include much higher thermal conductivity and electrical conductivity as well as lower cost. The eddy-current will be induced in the metallic sleeve instead of magnets. The metallic sleeve acts as the shield for harmonic penetration into the magnets. Nevertheless, the selection of retaining sleeve should not only consider the mechanical aspects such as the magnet protection but also the electromagnetic and thermal aspects including the rotor eddy-current loss reduction and rotor thermal issues.

In this paper, the retaining sleeve is selected to be the carbon-fibre due to its large tensile strength. At high-speed operation, the rotor components will suffer huge centrifugal force and certain amount of thermal stress. The PM material ideally has a high compressive strength (800MPa) and a medium flexural strength (120MPa), but it is rather brittle [11]. Hence, stress analysis is a key issue for the mechanical robustness of HSPMMs. The analysis of the rotor stress can be approximately

divided into two steps. Firstly, the exact value of stress in each rotor part should be **calculated**. **Secondly**, the maximum stress induced in each component of the rotor should be ensured within the material strength under all operating speed and temperature, especially for PMs which are quite vulnerable to tangential tensile stress. In addition, the contact pressure **between the PMs and the shaft** should always exist so that the electromagnetic torque can be transferred.

The methods for stress calculation can be classified into analytical and numerical ones. Several papers on analytical calculation of rotor stress can be found [6], [12]-[16]. [6] proposed a simplified analytical model for stress calculation based on the assumption that the rotor is strictly rotational symmetry. In [12] and [13], the displacement technique was adopted for the stress calculation of the HSPMM with the nonmagnetic alloy sleeve. In most of the analytical models, the PM rotors are normally modelled as the multi-layered cylinders. However, all the aforementioned analytical models are based on the assumption of planar stress which is valid for rotors with short axial length. Hence, in [14], a 3D analytical model considering the axial stress was established for both solid and hollow magnet rotors in the plane strain condition. Although all these analytical solutions are capable of providing a fundamental insight from the stress generation to reduction, as pointed out in [6], the **nonlinear factors** such as geometry discontinuity and edging effect cannot be considered in the analytical model. Hence, in order to obtain a more exact value of rotor stress, 2D or 3D finite-element methods (FEM) are more widely adopted in the calculation of rotor stress with complicated structure or other aforementioned strong **nonlinear factors**.

With the obtained stress in each component of the rotor, the priority is to ensure those **values** within the material limit in the whole operating speed and temperature range. Hence, it is essential to find the worst operating scenarios with respect to operating speed and temperature for each component of the rotor. The rotor stress is therefore checked only under the worst operating scenario instead of the whole working range. In fact, **quite few** papers have discussed about this issue. [6] pointed out the thermal expansion must be considered due to its significant portion in the sleeve tangential stress. However, how the rotor stress is affected by the temperature is not further studied. [8] comprehensively investigated the influence of operating speed and temperature on the sleeve and magnet tangential and radial stresses.

More importantly, all those mentioned findings are only valid for the PMs in an integral ring. **The potential influence of PM segmentation on the rotor stress values and worst operating scenarios are usually ignored in literature**. On the other hand, the influence of PM segmentation on the amplitude of rotor stress also remains to be investigated. It will be demonstrated in this paper that certain sleeve stress concentration will occur while the segmented magnets are under **the** tensile tangential stress. As a matter of fact, the stress concentration issue in the HSPMM with inter-pole gap has been reported in several papers. In [6], the inter-pole gap was removed in order to avoid the sleeve stress concentration. In [8], it was concluded that the

inter-pole filler significantly **reduces** the stress concentration in the retaining sleeve. In addition, the influence of material properties on the stress concentration mitigation effect was also revealed.

The main contributions of this paper can be summarized from two aspects. First of all, the phenomenon of stress concentration is firstly discovered in the retaining sleeve of high speed PM machines with segmented permanent magnets. The specific conditions and influential factors (e.g. number of segment, sleeve thickness...) are further identified. Hence, it can more clearly determine how to mitigate these localized stresses in the sleeve. Secondly, due to significant impact of retaining sleeve thickness on both the mechanical and electromagnetic performances, a new design scheme of sleeve thickness of high speed PM machines with segmented magnets is proposed based on the identified worst case scenarios. The relationship between the minimum sleeve thickness and the rotor outer diameter is calculated which can save the iteration processing time in the mechanical post-check of traditional design.

This paper is organized as follows. Firstly, in Section II, the phenomenon of sleeve stress concentration due to PM segmentation is revealed with 2D and 3D FE methods. The conditions for the presence of stress concentration are also determined. Then, in Section III, the influence of PM segmentation on the worst operating scenario is studied. Section IV investigates the influence of sleeve thickness and interference fit on the rotor stress while the PMs are segmented, providing a design guideline to avoid the presence of stress concentration by adjusting these two parameters. Based on the identified worst scenarios, a new design scheme of sleeve thickness is proposed in Section V. Finally, in Section VI, a 6-slot 4-pole high-speed PM machine with segmented magnets retained by carbon-fibre sleeve is prototyped and tested. The rotor runs safely at the speed of 90krpm. The conclusion is given in Section VII.

II. THEORETICAL ANALYSIS OF ROTOR STRESS WITH CARBON-FIBRE SLEEVE

In order to obtain the exact value of rotor stress in the HSPMM with carbon-fibre sleeve, in this section, the explicit 2D FE analysis of the rotor stress is conducted on a 4-pole high-power high-speed PM machine with the highest power and speed of 25kW and 100krpm, respectively. The rotor structural parameters and the material properties are given in Table I and Table II. The rotor thermal expansion and material anisotropy are considered. Then, the 2D FE predicted results are compared with the 3D FE predicted ones to verify the validity of the established model. **It should be noted that the deterioration effect factor 2.5 due to manufacturing is considered in the allowable material limit**. Hence, the tensile strength of carbon fibre sleeve is considered to be 1440MPa which is much lower than the value in the data sheet of carbon fibre material.

TABLE I MAIN PARAMETERS OF ROTOR GEOMETRY

Parameter	Symbol	Value
Pole pair number	p	2

Sleeve outer radius/mm	R_{so}	25
Sleeve inner radius /mm	R_{si}	22.5
Sleeve interference fit/mm	δ	0.25
PM outer radius /mm	R_{mo}	22.625
PM inner radius /mm	R_{mi}	15.125
Back-iron outer radius /mm	R_{bo}	15.125
Shaft radius /mm	R_{bi}	5
Stack length/mm	l	60

TABLE II MATERIAL PROPERTIES

Material	PM (NdFeB)	Carbon-fibre		Structural steel
		\perp	//	
Density/kg/m ³	7500	1790		7850
Young's Modulus/GPa	160	9.5	186	210
Poisson's ratio	0.24	0.018	0.31	0.3
CTE/ $\mu\text{m}/\text{m}/^\circ\text{C}$	8	35	0.02	10
Maximum allowable strength/MPa	Tensile 80	Tensile 1440		500

A. Rotor stress without PM segmentation

The rotor stress is calculated with a whole magnet ring or cylinder established in the FE models. Fig.2 shows the distribution of sleeve stress in the 2D and 3D FE models, respectively. It can be observed that the maximum sleeve stress occurs at the contact surface between the sleeve and the magnets due to the pre-stress introduced by the inference fit. In addition, the 2D FE predicted results match well with 3D FE predicted one, which indicates a negligible axial stress and therefore justifies the planar stress assumption in the 2D FE models. Hence, the 2D FE model can be accepted for the stress calculation in this case due to a much shorter computation time as well as an acceptable accuracy.

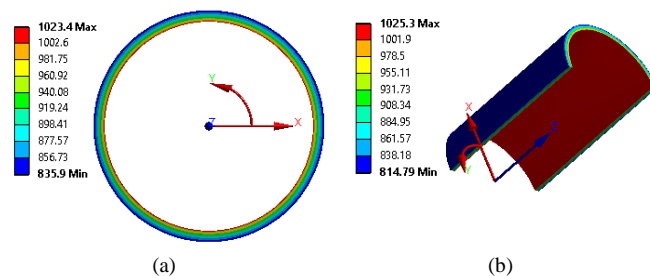


Fig.2. Sleeve tangential stress without magnet segmentation ($T=20^\circ\text{C}$ $n=100\text{krpm}$). (a) 2D. (b) 3D.

Table III COMPARISON OF DIFFERENT STRESS MODELS

Rotor stress (MPa)		Calculation models	
		2D-FEA	3D-FEA
Sleeve Tangential	$T=20^\circ\text{C}$	1023.4	1025.3
	$T=150^\circ\text{C}$	1214.5	1178
Sleeve Radial	$T=20^\circ\text{C}$	-88.4	-88.0
	$T=150^\circ\text{C}$	-112.3	-125.9
PM Tangential	$T=20^\circ\text{C}$	66.3	69.0
	$T=150^\circ\text{C}$	-23.2	-20.3
PM Radial	$T=20^\circ\text{C}$	0.15	0.20
	$T=150^\circ\text{C}$	0.04	0.07

B. Rotor stress considering PM segmentation

For high-speed PM machines, the metallic sleeve or the PMs are always segmented to reduce the rotor eddy-current loss [17], [18]. As has been mentioned, the rotor stress is mainly in the form of planar stress. Thus, in this section, the edging effect resulting from the circumferential segmentation is considered in the 2D FE model. It should be noted that except otherwise stated, the PM segmentations in this paper all refer to the circumferential segmentation.

The PM is established as a whole ring and eight individual segments in the 2D FE model, respectively, which corresponds to the different scenarios. The slits between segmented magnets are set to be 0.1mm. The potential contact condition is set to be frictional which means the displacements in the circumferential direction are allowed. The influence of segment number will be studied in Section IV. Fig.3 illustrates the variation of rotor tangential stress with operating speed with and without consideration of PM segmentation, respectively. The following observations can be concluded:

- 1) When the magnets are under the compressive tangential stress at a relatively lower operating speed, the magnet segmentation will not cause a significant difference in terms of rotor stress under this condition.
- 2) While the operating speed is relatively higher, the amplitude of PM tangential stress due to rotation exceeds the pre-tangential stress imposed by the retaining sleeve. The overall PM tangential stress tends to be tensile instead of compressive. As shown in Fig.3, the sleeve tangential stress will rise sharply with the increase of operating speed. Fig.4 shows the sleeve tangential stresses with and without magnet segmentation at 100krpm. The stress concentration does occur at the position aligned with edges of the magnets. When the magnets are under the tensile stress which increases significantly with the operating speed, the tangential displacement will become larger as well, as shown in Fig.6. Hence, the geometry discontinuity will be more serious. This deteriorates sleeve stress concentration which will be investigated individually in Section V.
- 3) Although the sleeve stress will increase significantly when the magnets are segmented and under the tangential tensile stress, the amplitude of PM tangential stress is reduced compared to that of an integral PM ring, as shown in Fig.3. This is because the gaps between the magnets provide a leak way for the travelling of tangential stress. Fig.5 shows the PM tangential stresses with and without PM segmentation at the speed of 100krpm. The hottest spot transfers from the inner side of PMs to the outer middle part. The maximum PM tangential stress is reduced from 66.3MPa to 21.9MPa.

In summary, for the rotors with segmented magnets, the edging effect must be considered in the FE models, especially when the PMs are under the tensile strength. Significant stress concentration will occur at the inner side of sleeve. On the contrary, the PMs themselves will benefit from the segmentation due to the presence of leak way.

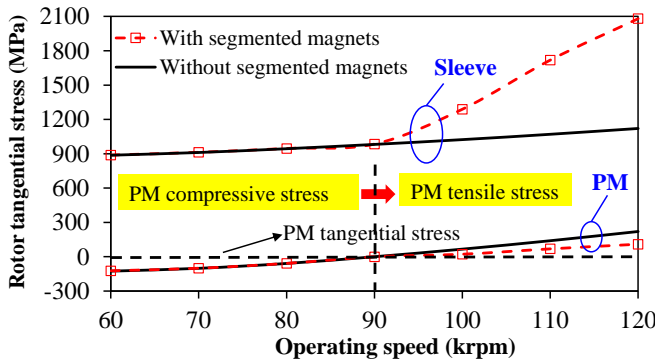


Fig.3. Variation of rotor tangential stresses with operating speed with/without magnet segmentation. ($T=20^{\circ}\text{C}$)

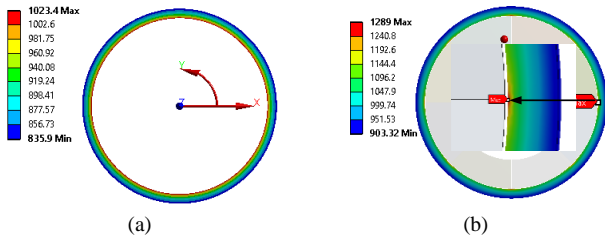


Fig.4. Sleeve tangential stress with and without magnet segmentation ($T=20^{\circ}\text{C}$ $n=100\text{krpm}$). (a) Without segmentation. (b) With segmentation.

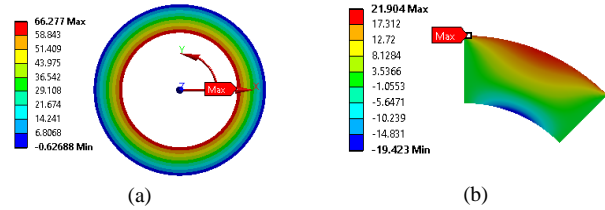


Fig.5. PM tangential stresses with and without magnet segmentation ($T=20^{\circ}\text{C}$ $n=100\text{krpm}$). (a) Without segmentation. (b) With segmentation.

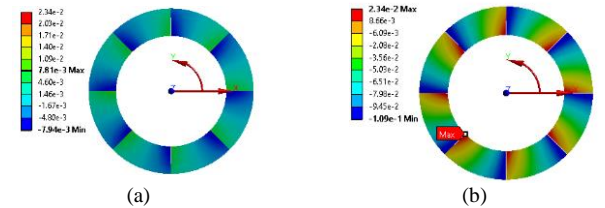


Fig.6. Variation of segmented PM tangential displacement with different operating speed ($T=20^{\circ}\text{C}$). (a) $n=90\text{krpm}$. (b) $n=120\text{krpm}$.

III. DETERMINATION OF WORST OPERATING SCENARIO CONSIDERING MAGNET SEGMENTATION

In the previous section, the influence of PM segmentation on the amplitude of rotor tangential stress has been determined. However, this is only applicable within a narrow speed range at a single rotor temperature. It remains unclear how the rotor stress will be affected by the magnet segmentation in the whole operating speed and rotor temperature range. Moreover, the rotor stress is also significantly influenced by the mechanical design parameters such as sleeve thickness and interference fit. Generally, the stress-impact factors can be classified into three groups, namely operating parameters, mechanical design parameters and geometric parameters. In real cases, the geometric parameters are firstly determined in the initial electrical design stage. With the geometric parameters obtained from the initial electrical design, the mechanical design can

thereby be conducted. The rotor stability check is normally conducted for different choices of mechanical design parameters such as interference fit and sleeve thickness. Fundamentally, the rotor mechanical stability conditions for a high-speed surface-mounted PM machine can be written as

$$\begin{cases} \text{Ref}[\sigma_{s,m}(r)] < \sigma_{\text{limit}}, \sigma_c < 0 \\ R_{bi} \leq r \leq R_{si}, 0 \leq \Omega \leq \Omega_{\text{max}}, T_{\text{min}} \leq T \leq T_{\text{max}} \end{cases} \quad (1)$$

where $\sigma_{s,m}$ denotes the tangential stress in the sleeve and rotor magnets; σ_c denotes the contact pressure between the rotor back iron and the rotor magnets. Ω refer to the operating speed and Ω_{max} denotes the maximum operating speed. T_{min} and T_{max} denote the minimum and maximum operating temperatures in the rotor.

As can be seen from (1), each rotating part in the rotor must be smaller than the yield strength or the tensile strength depending on the type of materials. For the carbon-fibre sleeve and PM investigated in this paper, the Tresca's criterion should be adopted. The tangential stresses of sleeve and magnet must be smaller than the material tensile strength. Meanwhile, the contact pressure between the magnets and the rotor back-iron must be negative in the cylindrical coordinate system, indicating that there is always a pressure pushing the PMs onto the back-iron so that the torque can be transferred. It should be noted that the aforementioned conditions should be fulfilled in the whole speed and rotor temperature range. Hence, it is necessary to identify the influence of operating speed and temperature on the rotor stress so that maximum rotor stress can be quickly obtained and the post-check of mechanical solutions can be more efficient. Hence, in this section, the worst operating scenarios concerning with the speed and temperature are determined with FE method, while the magnets are segmented.

A. Sleeve tangential stress

Fig.7 illustrates the variation of maximum sleeve tangential stress at the inner side of sleeve with operating speed and rotor temperature with and without consideration of PM segmentation. The following observations can be found:

- 1) While the magnets are under the compressive tangential stress, the maximum sleeve tangential stress increases significantly with the rise of operating speed and temperature, whenever the magnets are segmented. The sleeve tangential stress consists of pre-tangential stress, rotating tangential stress and thermal tangential stress. The latter two parts will increase with the rise of speed and rotor temperature. **The increase of speed and temperature will yield different level of displacements for the magnets and sleeve due to different material properties.** The actual interference fit will be significantly enlarged with the increase of speed and temperature compared to static one. This can be verified by the increase of sleeve inner side radial stress as shown in Fig.8. It can be seen that when the temperature rises from 20°C to 150°C , the sleeve radial stress at the inner side increases from 78.9MPa to 104MPa.
- 2) As has been proven in the previous section, the sleeve stress concentration will occur when the PM tangential stress turns to be tensile. Fig.7 (b) shows the variation of the

concentrated sleeve tangential stress with speed and temperature. There is no doubt that the stress will be increased with the rising speed. However, it is also interesting to see the concentrated sleeve tangential stress will be reduced with the increase of rotor temperature. This can be explained by the smaller gaps between PM segments when the temperature is higher. The PM tensile tangential stress will be reduced with the increase of rotor speed as will be shown in Fig.10. Hence, the deformation of the magnet edges will be correspondingly reduced. Fig.9 illustrates the tangential displacements of PMs under different rotor speed. The tangential displacement is significantly reduced by 78.11%.

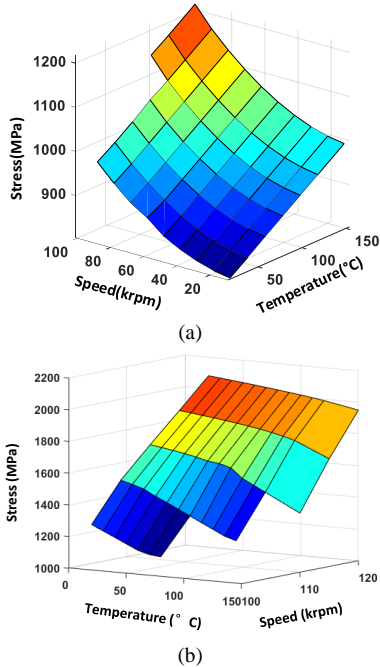


Fig.7. Variation of maximum sleeve tangential stress with operating speed and rotor temperature with/without PM segmentation. (a) PMs under compressive tangential stress. (b) Segmented PMs under tensile tangential stress.

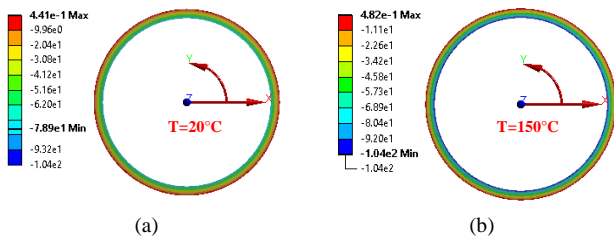


Fig.8. Distribution of sleeve radial stress with PMs withstanding compressive tangential stress ($n=30$ krpm). (a) $T=20^{\circ}\text{C}$. (b) $T=150^{\circ}\text{C}$.

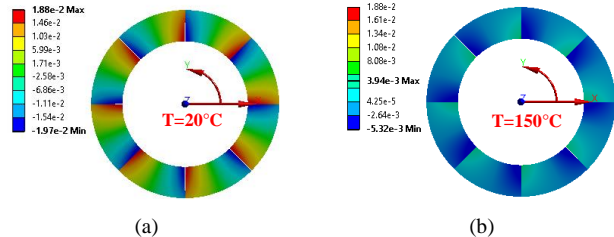


Fig.9. Tangential displacements of PMs withstanding tensile tangential stress ($n=100$ krpm). (a) $T=20^{\circ}\text{C}$. (b) $T=150^{\circ}\text{C}$.

B. PM tangential stress

Fig.10 illustrates the variation of maximum PM tangential stress with operating speed and rotor temperature. Similarly, the value will be maximum at the maximum operating speed, regardless of the magnet segmentation. In contrast, the maximum PM tangential stress will be significantly reduced with the increasing temperature. The maximum PM tangential stress is reached at the maximum operating speed and lowest rotor temperature. As mentioned in the previous section, the interference fit will be increased when the rotor temperature becomes higher thus resulting a larger radial stress and compressive tangential stress on the rotor magnets. Hence, the tensile PM tangential stress resulting from high speed rotating is partially cancelled by the compressive PM tangential stress imposed by the retaining sleeve.

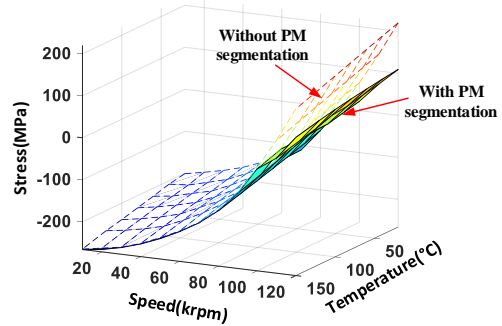


Fig.10. Variation of maximum PM tangential stress with operating speed and rotor temperature with and without PM segmentation.

On the other hand, while the PMs are segmented, the maximum tensile PM tangential stress will be significantly reduced due to the presence of leak way between the segmented magnets, which is beneficial to the rotor mechanical stability.

C. Contact pressure between magnets and back-iron

Fig.11 shows the variation of contact pressure with operating speed and rotor temperature. It can be seen that the maximum contact pressure occurs at maximum operating speed and minimum rotor temperature. It shares the same trend with the PM tangential stress. In addition, the PM segmentation will yield a larger contact pressure while the PMs are under tensile strength.

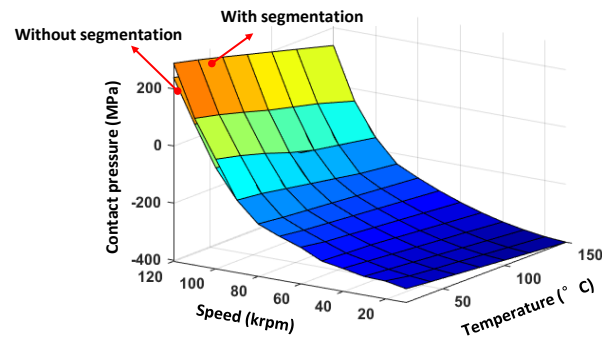


Fig.11. Variation of contact pressure with operating speed and rotor temperature with/without PM segmentation.

Table IV summarizes the worst operating scenarios with and without consideration of PM segmentation. It is obvious that the worst case always occurs at the maximum speed whenever the

magnets are segmented. While the magnets are not segmented, the worst case for the sleeve tangential stress occurs at the highest rotor temperature. By contrast, the worst cases for PM tangential stress and contact pressure occur at the lowest rotor temperature. While the magnets are segmented, the worst cases for the PM tangential stress and contact pressure keep the same. However, the worst case for sleeve tangential stress remains stable only when the PMs are under compressive stress. When the segmented PMs are under tensile stress, the worst case for sleeve tangential stress occurs at the lowest rotor temperature which is opposite to that of unsegmented condition.

On the other hand, although the PM tangential stress can be reduced significantly when it is under the tensile stress. However, **simultaneously**, it also causes the stress concentration in the retaining sleeve. Moreover, the risk of loose of contact is increasing. Hence, the machine designers should keep the segmented PMs under the compressive state as much as possible to avoid sleeve stress concentration. Even when the magnets must be under the tensile state, special attention should be made to ensure the maximum concentrated sleeve tangential stress smaller than the tensile strength of sleeve at the maximum speed and the lowest rotor temperature.

Table IV WORST OPERATING SCENARIOS WITH AND WITHOUT PM SEGMENTATION

Rotor stress		Speed n		Temperature T	
		W/O SEG	W/ SEG	W/O SEG	W/ SEG
Sleeve Tangential	PM CS	Max.	Max.	Max.	Max.
	PM TS	Max.	Max.	Max.	Min.
PM Tangential		Max.	Max.	Min.	Min.
Contact pressure		Max.	Max.	Min.	Min.

Note: W/SEG and W/O SEG designate for with and without segmentation. PM CS and PMTS designate for PM compressive stress and tensile stress.

IV. INFLUENCE OF MECHANICAL DESIGN PARAMETERS ON ROTOR STRESS

The worst operating case of high-speed PM machine considering the magnet segmentation has been determined in the previous section. However, the rotor stress is also significantly influenced by the mechanical design parameters such as sleeve thickness and interference fit. In addition, the geometry parameters such as PM thickness and rotor split ratio also have a great impact on the exact value of rotor stress which has been discussed in [19]-[21]. Hence, in this section, the influence of sleeve thickness and interference fit on the rotor stress considering the PM segmentation is investigated. The guideline on the appropriate selection of those parameters will be given so that the stress concentration can be avoided. Another factor should be considered is the number of PM segments. Although the influence of PM segment number has been discussed in a variety of papers, all the investigations focus on the PM eddy-current loss reduction only. Hence, the influence of PM segment number on the rotor stress will also be addressed in this section.

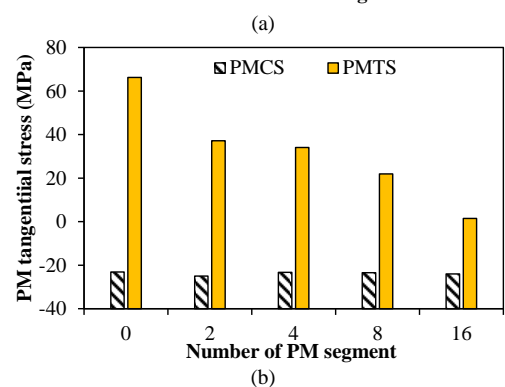
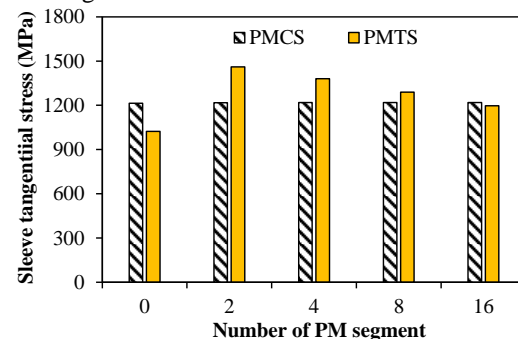
A. Number of PM segment

Fig.12 illustrates the variation of rotor stress with the number of PM segments in two different scenarios. While the segmented PMs are under compressive stress (PMCS), the rotor stress almost keeps stable despite of the change of PM segment number. However, while the PMs are under tensile stress (PMTS), the number of PM segments has a great impact on the rotor stress.

For the sleeve tangential stress, although a significant increase of amplitude can be observed due to the presence of stress concentration in all the inner side of sleeve with different PM segment number, it is decreased with increase of PM segment number. The increase of PM segment number weakens the edging effect of segmentation. Fig.13 shows the tangential displacements of segmented PMs under tensile tangential stress. It is obvious when the segment number increases from 2 to 8, the maximum tangential displacement decreases by 42.3%.

On the other hand, the PM tangential stress and contact pressure also benefit from the increase of PM segment number. Both the PM tangential stress and contact pressure decrease significantly with the rise of number of PM segments.

In real cases, the increase of PM segment number will increase the manufacturing difficulties. A trade-off should be made between reducing the rotor stress, loss and increasing the manufacturing difficulties.



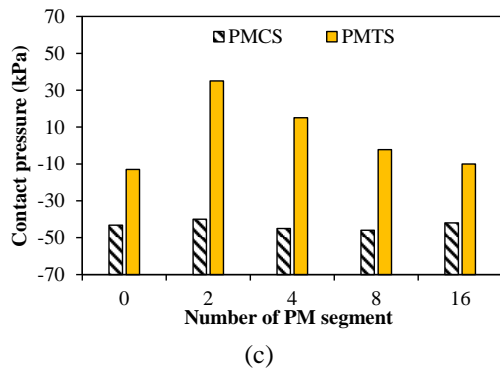


Fig. 12. Influence of PM segment number on the rotor stress. (a) Sleeve tangential stress. (b) PM tangential stress. (c) Contact pressure between PM and rotor yoke.

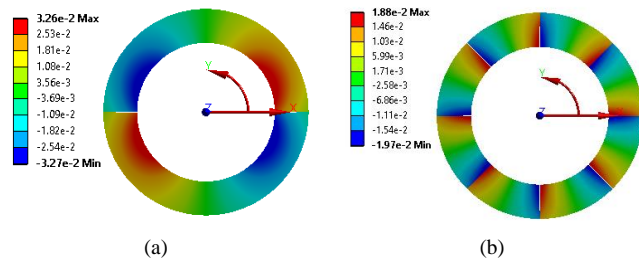


Fig. 13. Tangential displacements of segmented PMs withstanding tensile tangential stress. (a) $N=2$. (b) $N=8$.

B. Sleeve thickness and interference fit

As pointed out in [6], the sleeve thickness H_b and interference fit determine the pre-stress imposed on the rotor magnets. In this section, the influence of sleeve thickness and interference fit on the rotor stress considering the PM segmentation is investigated.

Fig. 14 illustrates the variation of rotor stress with sleeve thickness and interference fit. It can be seen that the increasing sleeve thickness will significantly reduce the sleeve tangential stress, the PM tangential stress and the contact pressure in the whole interference fit range. More importantly, the increase of sleeve thickness reduces the minimum interference fit beyond which the PM tangential stress tends to be compressive (less than zero). In other words, the maximum operating speed at which the PM tangential stress is compressive can be increased within given interference fit.

However, from the electromagnetic point of view, the equivalent air gap thickness will be increased simultaneously, yielding a lower air gap flux density which may decrease the torque density. Hence, a trade-off should be made between the reduction of rotor stress and torque density by increasing the sleeve thickness.

On the other hand, within given sleeve thickness, both the PM tangential stress and contact pressure are significantly reduced with the increase of interference fit. This should be attributed to the increase of pre-stress imposed on the PMs. However, for the sleeve tangential stress, it keeps decreasing before reaching the minimum value at a certain interference fit. Then, it starts to rise with the increase of interference fit. When the interference fit is relatively small, the PMs are under tensile stress as shown in Fig. 15(b). The stress concentration occurs at the inner side of sleeve due to magnet edging effect. This effect is eased when the interference fit becomes larger due to the

reduction of segmented PM tangential tensile stress. Hence, the sleeve stress concentration effect is weakened. While the segmented PMs are under the tangential compressive stress, the sleeve stress concentration disappears. The main component of sleeve tangential stress is the pre-stress due to the interference fit. Hence, it increases significantly with the enlarged interference fit.

To conclude, for the mechanical design of rotor sleeve, on one hand, the sleeve stress concentration due to segmented magnet edging effect can be avoided by choosing a relatively larger interference fit whose minimum value can be reduced by increasing the sleeve thickness. What is more, the PMs are under compressive stress and the contact pressure is maintained for the torque transfer under this circumstance. On the other hand, it should also bear in mind the sleeve tangential stress may exceed the material tensile strength if the interference fit becomes too high. In addition, the maximum value of interference fit is also limited by the sleeve outer diameter and CTE when the retaining sleeve is cold-shrunk onto the segmented PMs.

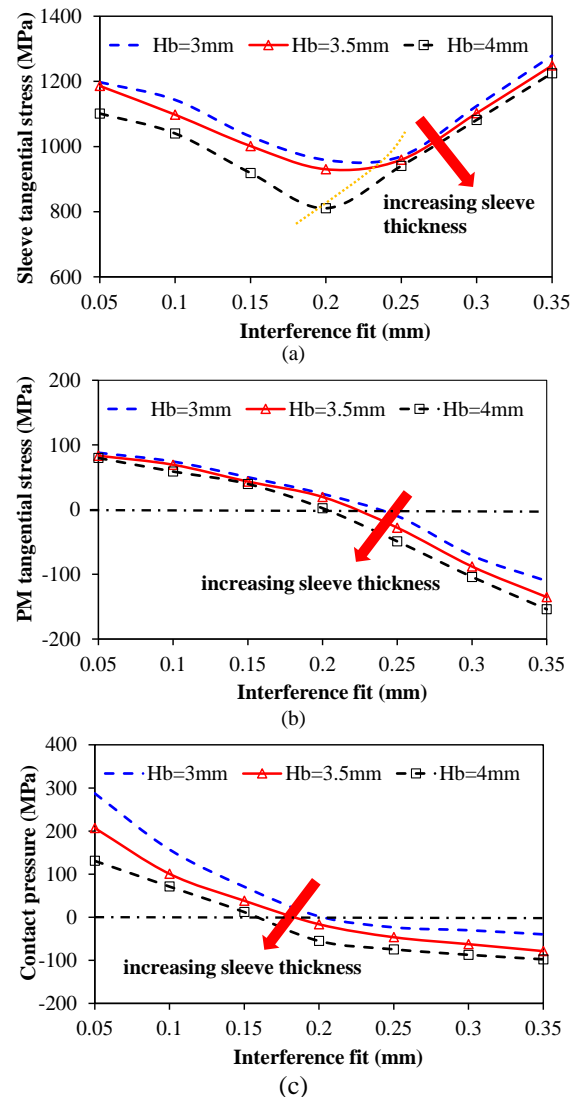


Fig. 14. Influence of sleeve thickness and interference fit on the rotor stress. (a) Sleeve tangential stress. (b) PM tangential stress. (c) Contact pressure between PM and rotor yoke.

V. DETERMINATION OF MINIMUM RETAINING SLEEVE THICKNESS CONSIDERING MAGNET SEGMENTATION

As has been demonstrated in Section IV, the rotor stability can be effectively enhanced with the increasing sleeve thickness. However, the effective air gap length will be inevitably increased due to the presence of retaining sleeve. The air gap flux density will thereby be reduced, resulting in a lower output torque/torque density. Hence, the appropriate design of sleeve thickness is quite important for both the mechanical and electromagnetic performance. In this section, a new design scheme for the sleeve thickness is proposed. The minimum sleeve thickness with variation of rotor diameter is determined based on the identified worst case scenarios in Section III.

It was pointed out in [20] that the feasible selection of sleeve thickness is inter-dependent on the value of rotor diameter. There exists a minimum sleeve thickness for specific rotor geometry with given PM thickness and rotor outer diameter. However, the thermal stress was ignored in the stress analysis. More importantly, the magnet segmentation could not be considered in the analytical calculation of rotor stress and thus may lead to the derivation of the actual sleeve and PM tangential stresses. Hence, in this section, with the identified worst case scenarios considering the magnet segmentation, the feasible variation of rotor diameter with sleeve thickness is determined through 2D FE parametric analysis.

Fig. 15 illustrates the variation of rotor stress including sleeve and PM tangential stresses as well as contact pressure with rotor outer diameter and sleeve thickness under the identified worst working scenarios. On one hand, there is no doubt that the smallest sleeve thickness will yield the maximum rotor stress within a given rotor diameter. On the other hand, it can be seen that both the maximum PM tangential stress and the minimum contact pressure occur at the geometry with the maximum rotor outer diameter and the smallest sleeve thickness. However, for the sleeve tangential stress, there exists a unique rotor outer diameter at which the value of stress reaches the minimum within a given sleeve thickness. This phenomenon is also confirmed in [20]. This can be explained by different trends of sleeve tangential stress components with the enlarged rotor diameter. In [6], it was pointed that sleeve tangential stress consists of pre-stress due to the shrink-fit between the sleeve and the rotor magnets and the rotation stress. The pre-stress is reduced with the increase of rotor diameter in the hyperbolic trend due to the decreasing strain. Since the rotation tangential stress is proportional to the square of rotor diameter, the sleeve tangential stress starts to decrease with the increase of rotor diameter due to the dominating pre-stress reduction effect. When the rotor diameter becomes larger, the pre-stress tends to be stable. However, the sleeve tangential stress due to rotation increases significantly with the rotor outer diameter. Hence, the resultant sleeve tangential stress becomes larger.

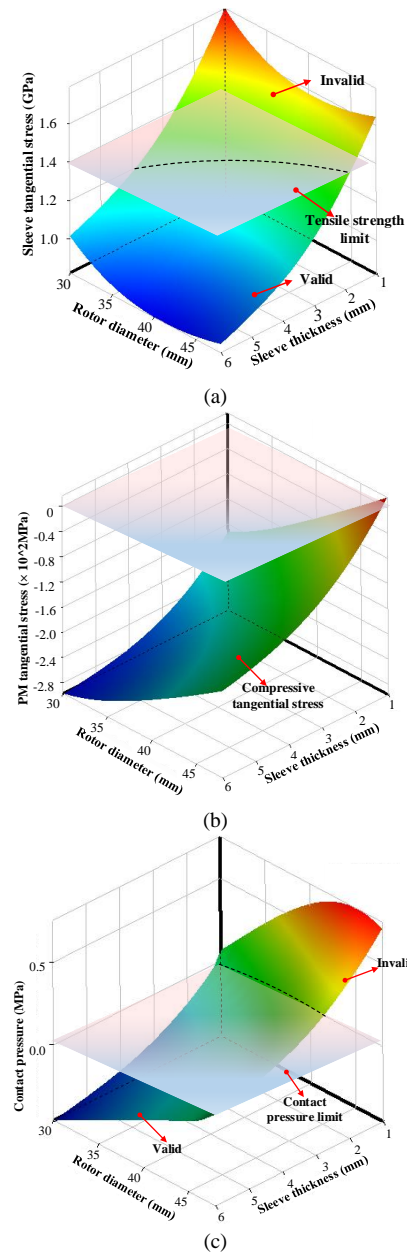


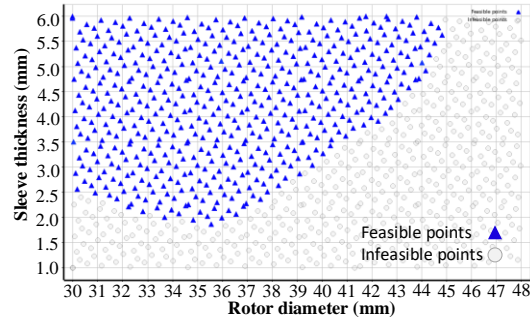
Fig. 15. Variation of rotor stress with rotor diameter and sleeve thickness at worst-operating scenario. (a) Maximum sleeve tangential stress. (b) Maximum PM tangential stress. (c) Contact pressure between PM and rotor back-iron.

According to the aforementioned conditions for rotor non-failure of HSPMM, the stress limitation surfaces are placed in Fig. 15. It can be seen from Fig. 15 (a) that the lower part of surface is valid. There are three intersections created by six surfaces. When those intersections are projected into the 2D plane (X-Y plane), the valid selection of rotor diameter and sleeve thickness can thereby be obtained as shown in Fig. 16. It should be noted that although the PM tensile stress limit is 80MPa, the limitation surface is set to be 0MPa to ensure the PMs are under compressive tangential stress so that the stress concentration can be avoided when the PM segmentation is adopted.

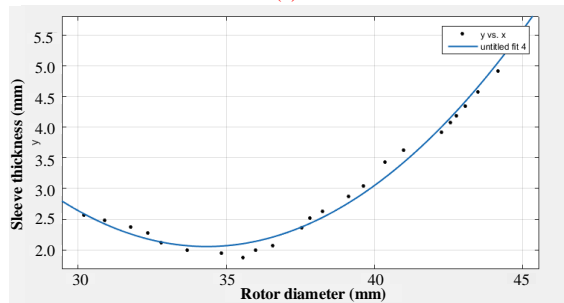
With the help of curve-fitting tool in MATLAB, the minimum sleeve thickness with respect to the rotor diameter considering the rotor mechanical integrity can be written as:

$$H_b \geq k_1 R_{mo}^3 + k_2 R_{mo}^2 + k_3 R_{mo} + k_4 \quad (2)$$

where k_1, k_2, k_3, k_4 are the coefficients which highly depend on the permanent magnet thickness, interference fit, retaining sleeve and permanent magnet material as well as maximum operating speed and rotor temperature. With the help of the proposed scheme, the iterations can be saved in the traditional post-check of mechanical design. In addition, the real optimal solution with higher torque density can be found more efficiently in the electromagnetic design without worrying about its mechanical validity.



(a)



(b)

Fig.16 Feasible variation of sleeve thickness with rotor diameter considering mechanical stress constraints. (a) Pareto fronts. (b) Curve-fitted constraints for rotor diameter and sleeve thickness.

VI. PROTOTYPE MACHINE FABRICATION AND TEST

Based on the previous design guideline, a three-phase, 6-slot/4-pole high speed machine with segmented permanent magnets retained by carbon-fibre sleeve is prototyped. The rated power is 25kW and rated operating speed is 65krpm. The maximum operating speed is 100krpm. The specifications of the prototype machine are given in Table V.

TABLE V MAIN PARAMETERS OF PROTOTYPE MACHINE

Parameter	Value
Slot number	6
Pole pair number	2
Stator outer diameter/mm	90
Stator bore diameter/mm	45.9
Stator yoke/mm	6.4
Tooth width/mm	7.7
Tooth opening/mm	3.96
Air gap length/mm	1
Sleeve thickness /mm	3
PM outer diameter /mm	37.9
PM inner diameter /mm	25.9

Pole arc to pole pith ratio	1
Shaft diameter /mm	8
Serial number of turns per phase	16
Stack length/mm	55

A. Fabrication

As shown in Fig.17 (a), the permanent magnets are circumferentially segmented into four pieces. The pole arc to pole pitch ratio is designed to be 1 so that the localised stress can be avoided at the inter-pole position. In addition, the PM outer diameter is designed to be 37.9mm from the electromagnetic point of view. According to the relationship between the minimum sleeve thickness and the rotor outer diameter shown in Fig.16 (b), the sleeve thickness is finally chosen to be 3mm so that the PM tangential stress is kept negative at the maximum operating speed and room temperature. The retaining sleeve is made of the prefabricated carbon fibre as shown in Fig.17 (b). The sleeve is axially pressed onto the rotor glued with segmented magnets as shown in Fig.17 (c), so that the pre-contact stress can be established between the sleeve and the magnets. In order to achieve the maximum operating speed, the hybrid deep groove ball bearings with rubber seal on both sides are selected as shown in Fig.17 (d). Fig.17 (e) shows the stator assembly of the prototype machine. Fig.17 (f) shows the rotor assembly whose balancing was done by drilling holes in the end copper rings at both sides of the rotor.

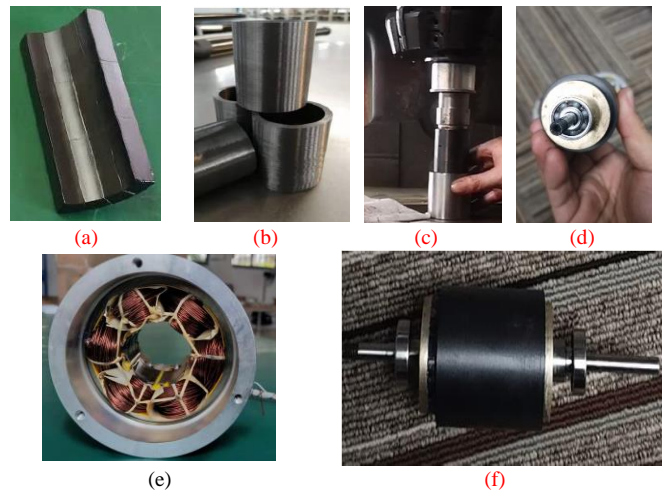


Fig.17. Fabrication and components of high speed permanent magnet machine. (a) Segmented magnets. (b) Prefabricated carbon fibre. (c) Axial pressing of carbon fibre sleeve. (d) Bearing. (e) Stator assembly. (f) Rotor assembly.

B. Test

For the open-circuit test, the back-EMF was tested at different operating speed. The prototype machine is driven by the dynamometer shown in Fig. 18(b). The measured and simulated open-circuit back-EMFs and corresponding spectra are shown in Fig.19 and Fig.20. Although there is a 10% difference between the measured and predicted data, the good agreement can be observed. This discrepancy can be attributed to the ignorance of end effect in the FE model. On the other hand, with significant amount of the 5th and 7th harmonics, the

back-EMF waveform of the prototype machine is closer to a trapezoidal waveform.

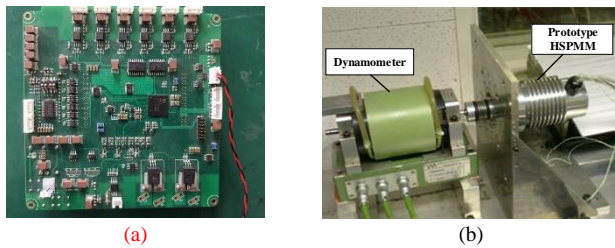
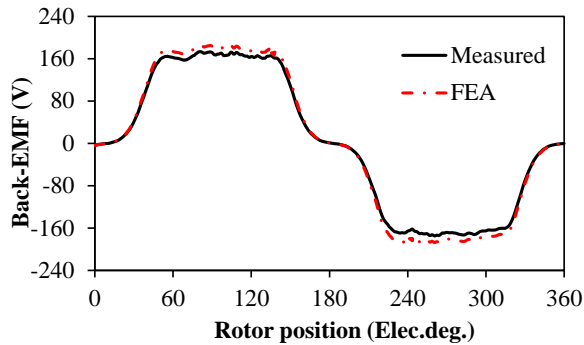
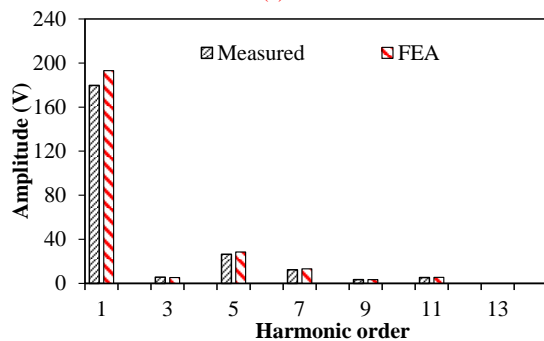


Fig.18. Test rig and drive. (a) Motor drive. (b) Test rig.



(a)



(b)

Fig.19. Measured and simulated back-EMF waveforms and spectra at 90krpm. (a) Back-EMF. (b) Spectra.

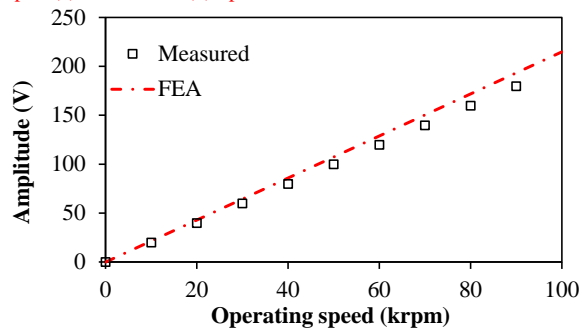


Fig.20. Variation of amplitude of EMF fundamental component with operating speed.

For the on-load test, due to the limited capacity of the inverter and control algorithm, the motor is driven to 90krpm with the light load (25A) by the controller. Fig.21 shows the current waveform of Phase A under the unmodulated six step control at the speed of 90krpm. On the other hand, in order to verify the rotor stability, the long-time duration operation is conducted at the speed of 90krpm with the current 25A. The temperature on the housing is measured every 5 minutes by the thermometer. Fig.22 shows the variation of temperature with time. It is obvious the thermal equilibrium is reached at the light

load condition. More importantly, the safe running of the rotor indicates the designed sleeve and segmented permanent magnet are capable of withstanding the huge mechanical stress at such a high operating speed.

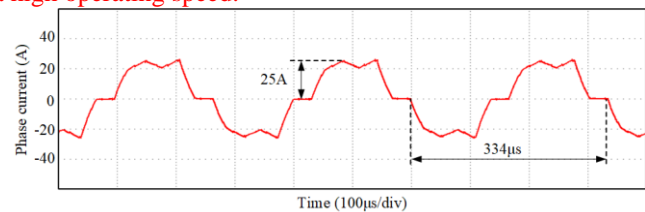


Fig.21. Measured Phase A current waveform under the unmodulated six step control at the speed of 90krpm.

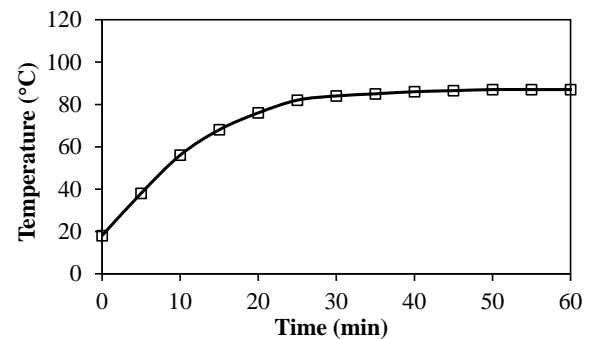


Fig.22. Measured temperature at the speed of 90krpm.

VII. CONCLUSION

In this paper, the rotor stress is analysed for a high-speed PM machine with segmented magnets retained by carbon-fibre sleeve. The rotor PM segmentation is firstly considered in the stress analysis of high-speed PM machines. It is shown that significant sleeve tangential stress concentration will occur when the segmented magnets are under tensile tangential stress. On the other hand, the PM tangential stress will be reduced when the segmentation is adopted. In addition, with the increase of segment number, this sleeve stress concentration effect is weakened whilst the PM tangential stress reduction effect is enhanced. Increasing sleeve thickness and interference fit can be adopted to avoid the stress concentration effectively. Meanwhile, the influence of PM segmentation on the worst operating scenario is determined. It is shown that the maximum concentrated sleeve stress occurs at the minimum operating temperature instead of the maximum temperature for the one without PM segmentation. A new design scheme of sleeve thickness is proposed based on the identified worst case scenarios. Finally, a 6-slot 4-pole high speed PM machine with segmented magnets retained by carbon-fibre sleeve is prototyped and tested at the speed of 90krpm. The rotor stability indirectly indicates the validity of the theoretical analysis and design scheme.

REFERENCES

- [1] F. Zhou, J. X. Shen, W. Fei, and R. Lin, "Study of retaining sleeve and conductive shield and their influence on rotor loss in high-speed PM BLDC motors," *IEEE Trans. Magn.*, vol. 42, no. 10, pp. 3398–3400, Oct. 2006.
- [2] C. Zwysig, J. W. Kolar, W. Thaler, and M. Vohrer, "Design of a 100W, 500 000 rpm permanent-magnet generator for mesoscale gas

- turbines," in *Proc. IEEE IAS Ind. Appl. Soc. 40th Annu. Meeting*, CD, Oct. 2005.
- [3] P.D.Pfister and Y. Perriard, "Very-high-speed slotless permanent magnet motors: Analytical modeling, optimization, design, and torque measurement methods," *IEEE Trans. Ind. Electron.*, vol. 57, no. 1, pp. 296–303, Jan. 2010.
- [4] D. K. Hong, B. C. Woo, J. Y. Lee, and D. H. Koo, "Ultra high speed motor supported by air foil bearings for air blower cooling fuel cells," *IEEE Trans. Magn.*, vol. 48, no. 2, pp. 871–874, Feb. 2012.
- [5] S. M. Jang, H. W. Cho, S. H. Lee, H. S. Yang, and Y. H. Jeong, "The influence of magnetization pattern on the rotor losses of permanent magnet high-speed machines," *IEEE Trans. Magn.*, vol. 40, no. 4, pp. 2062–2064, 2004.
- [6] A. Binder, T. Schneider, and M. Klohr, "Fixation of buried and surface-mounted magnets in high-speed permanent-magnet synchronous machines," *IEEE Trans. Ind. Appl.*, vol. 42, no. 4, pp. 1031–1037, Jul./Aug. 2006.
- [7] F. Luise, A. Tassarolo, F. Agnolet, S. Pieri, M. Scalabrin, and P. Raffin, "A high-performance 640-kW 10000-rpm Halbach-array PM slotless motor with active magnetic bearings. Part II: Manufacturing and testing," in *Proc. Int. Symp. Power Electron., Elect. Drives, Autom. Motion (SPEEDAM)*, Jun. 2014, pp. 1245–1250.
- [8] F. Zhang, G. Du, T. Wang, G. Liu, and W. Cao, "Rotor retaining sleeve design for a 1.12 MW high-speed PM machine," *IEEE Trans. Ind. Appl.*, vol. 51, no. 5, pp. 3675–3685, Sep./Oct. 2015.
- [9] W. Li, H. Qiu, X. Zhang, J. Cao, S. Zhang, and R. Yi, "Influence of rotor-sleeve electromagnetic characteristics on high-speed permanent-magnet generator," *IEEE Trans. Ind. Electron.*, vol. 61, no. 6, pp. 3030–3037, 2014.
- [10] M. R. Shah and A. M. EL-Refaie, "Eddy current loss minimization in conducting sleeves of high speed machine rotors by optimal axial segmentation and copper cladding," *IEEE Trans. Ind. Appl.*, vol. 45, no. 2, pp. 720–728, Mar./Apr. 2009.
- [11] Z. Huang and J. Fang, "Multiphysics design and optimization of high-speed permanent-magnet electrical machines for air blower applications," *IEEE Trans. Ind. Electron.*, vol. 63, no. 5, pp. 2766–2774, May.2016.
- [12] T. Wang, F. Wang, H. Bai, and J. Xing, "Optimization design of rotor structure for high-speed permanent-magnet machines," in *Proc. Int. Conf. Elect. Mach. Syst.*, 2007, pp. 1438–1442.
- [13] A. Borisavljevic, H. Polinder, and J. A. Ferreira, "On the speed limits of permanent-magnet machines," *IEEE Trans. Ind. Electron.*, vol. 57, no. 1, pp. 220–227, 2010.
- [14] G. Burnand, D. M. Araujo, and Y. Perriard, "Very-high-speed permanent magnet motors: Mechanical rotor stresses analytical model," in *2017 IEEE International Electric Machines and Drives Conference (IEMDC)*, 2017, pp. 1–7.
- [15] F. Chai, Y. Li, P. Liang and Y. Pei, "Calculation of the Maximum Mechanical Stress on the Rotor of Interior Permanent-Magnet Synchronous Motors," *IEEE Trans. Ind. Electron.*, vol. 63, no. 6, pp. 3420–3432, Jun. 2016.
- [16] S. Wu, X. Huang, L. He, S. Cui and W. Zhao, "Mechanical strength analysis of pulsed alternator air-core rotor," *IEEE Trans. Plasma Sci.*, vol. 47, no. 5, pp. 2387–2392, May 2019.
- [17] J.X. Shen, H. Hao, M.J. Jin, and C. Yuan, "Reduction of rotor eddy current loss in high speed PM brushless machines by grooving retaining sleeve," *IEEE Trans. Mag.*, vol. 49, no. 7, pp. 3973–3976, 2013.
- [18] K. Yamazaki, M. Shina, Y. Kanou, M. Miwa, and J. Hagiwara, "Effect of eddy current loss reduction by segmentation of magnets in synchronous motors: Difference between interior and surface types," *IEEE Trans. Magn.*, vol. 45, pp. 4756–4759, Oct. 2009.
- [19] G. Du, W. Xu, J. Zhu and N. Huang, "Rotor stress analysis for high-speed permanent magnet machines considering assembly gap and temperature gradient," *IEEE Trans. Energy Convers.*, vol. 34, no. 4, pp. 2276–2285, Dec. 2019.
- [20] J. H. Feng, Y. Wang, S. Y. Guo, Z. C. Chen, Y. Wang, Z. Q. Zhu, "Split ratio optimisation of high-speed permanent magnet brushless machines considering mechanical constraints", *IET Electric Power Applications*, vol. 13, no. 1, pp. 81–90, 2019
- [21] G. Du, W. Xu, J. Zhu, and N. Huang, "Effects of design parameters on the multi-physics performance of high-speed permanent magnet machines," *IEEE Trans. Ind. Electron.*, vol. 67, no. 5, pp. 3472–3483, May 2020.

- [22] G. Qi, J. T. Chen, Z. Q. Zhu, D. Howe, L. Zhou, and C. Gu, "Influence of skew and cross-coupling on flux-weakening performance of permanent-magnet brushless AC machines," *IEEE Trans. Magn.*, vol. 45, no. 5, pp. 2110–2117, May 2009.

APPENDIX

A. Demagnetisation withstand capability

The PM demagnetisation withstand capability is investigated in this section. The working condition is considered as three-phase short-circuit which is obtained in Motor-CAD. As shown in Fig.23 (a), a significant amount of transient demagnetisation current occurs in the D-axis. Fig.23 (b) illustrates the radial flux density in the PMs with different segment number. It can be seen that the more areas are being demagnetised at the edges of magnets without segmentation. The magnet segmentation slightly enhances the demagnetisation withstand capability due to the increase of reluctance brought by the segmentation gaps.

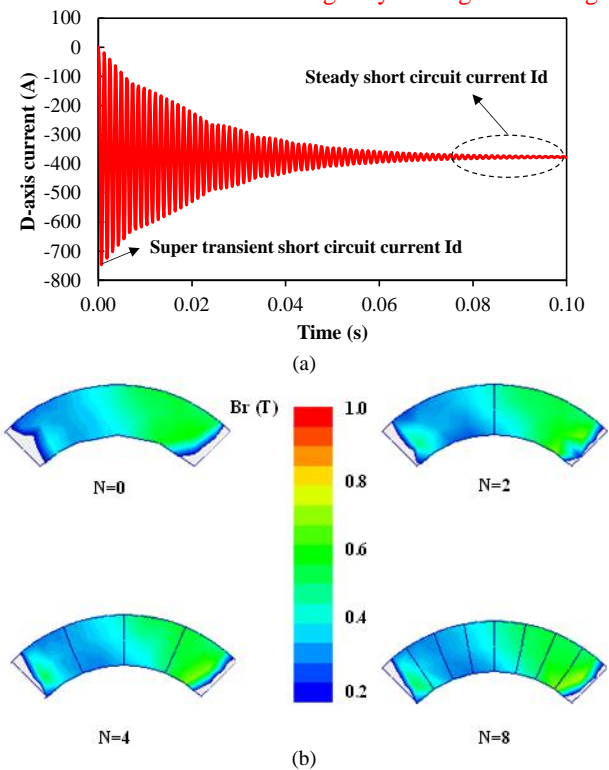


Fig.23. Demagnetisation analysis of high speed PM machines in Motor-CAD. (a) Three-phase short-circuit current. (b) Radial flux density of the magnets.

B. Flux weakening capability

The dynamic characteristics of the investigated high speed PM machines with and without segmentation are shown in Fig. 24. The FE-predicted torque-speed curves are calculated with the help of ANSYS and MATLAB software based on [22]. It can be seen that the magnet segmentation have no obvious impact on the flux weakening performances. This can be explained the d-axis inductance remains stable regardless of the magnet segmentation. In addition, the influence of fringing effect on the d-axis flux linkage is negligible.

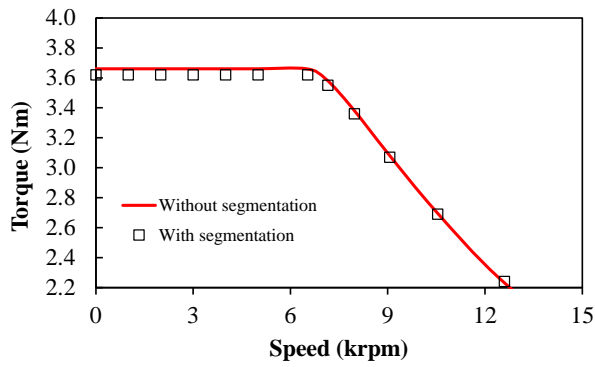


Fig.24. Torque-speed curve of the investigated high speed PM machines.

C. Thermal performance

The thermal performance of the prototype machine is investigated in this section. The prototype machine is enclosed with a water jacket as shown in Fig.25 (a). Fig.25 (b) shows the thermal distribution in the axial direction. It can be seen that the hottest spot in the stator occurs at the end-winding, reaching 144.4° C. While in the rotor, the temperature in the magnets has reached 139.4° C.

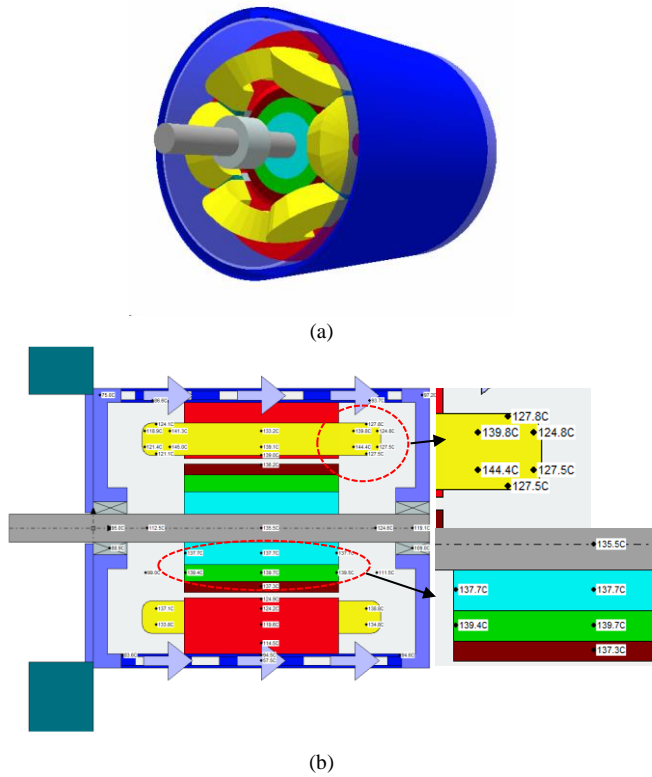


Fig.25. Thermal analysis of high speed PM machines. (a) Thermal model in Motor-CAD. (b) Thermal distribution.

Manuscript Title: Rotor Stress Analysis of High-Speed Permanent Magnet Machines with Segmented Magnets Retained by Carbon-Fibre Sleeve

Paper ID: TEC-00226-2020

Dear Editor:

Thank you for your and the reviewers' very constructive comments on our manuscript. We have taken all the comments and suggestions carefully in our revision. The detailed modifications and explanations are described in the response letter. All of the revisions have been highlighted with red in the revised manuscript.

Yours faithfully,

Prof. Z. Q. Zhu

Department of Electronic and Electrical Engineering

University of Sheffield,

Mappin Street, Sheffield S1 3JD, UK

AE Comments to the author

The reviewers have identified significant issues, the most important of which include more carefully establishing the novelty of the contribution, some presentation issues, and the suitability of the experimental results for validation. These must be carefully addressed for the paper to warrant further consideration. As is commonly expected, the authors should prepare a point-by-point response to the points raised by the reviewers and clearly indicate (e.g., in another color) modifications to the manuscript necessary to address the reviewers' concerns.

Response:

Thanks a lot for your constructive comments. We have tried our best to improve the quality of our manuscript by taking all reviewers' comments and suggestions into consideration. We have done the following work in order to address the mentioned three major issues as follows:

1. The novelty of the contribution

Thank you for your comment. We add the following in the introduction part to make the novelty of our work more clear: "The main contribution of the paper can be summarized from two aspects. First of all, the phenomenon of stress concentration is firstly discovered in the retaining sleeve of high speed PM machines with segmented permanent magnets. The specific conditions and influential factors (e.g. number of segment, sleeve thickness...) are then identified. Hence, it can more clearly determine how to mitigate this localized stress in the sleeve. More importantly, due to the significant impact of retaining sleeve thickness on both the mechanical and electromagnetic performances, a new design scheme of sleeve thickness of high speed PM machines with segmented magnets is proposed based on the findings on the worst case scenarios. The relationship between the minimum sleeve thickness and the rotor outer diameter is calculated which can save the time-consuming iteration processing time in the post-check of traditional mechanical design." In order to better explain this proposed new design scheme, we add a separate section (**Section V**) to discuss how to calculate the minimum sleeve thickness. The proposed scheme of sleeve design is quite important for the electromagnetic and mechanical design of high speed

1
2
3 PM machines. More importantly, compared with conventional design methods, it is more efficient and
4 provides more insight for investigating the coupled multi-physics mechanism in high speed PM
5 machines. With the help of the proposed scheme, the iterations can be eliminated in the traditional post-
6 check of mechanical design. In addition, the real optimal solution with higher torque density can be found
7 more efficiently in the electromagnetic design without worrying about its mechanical validity. We also
8 add the details of this part in the abstract and conclusion. We hope these two mentioned aspects have
9 addressed your concerns.
10
11
12

13 14 **2. Suitability of the experimental results**

15 We are really sorry the weak experimental validation in the previous manuscript. In order to validate the
16 rotor stability at a higher speed, we strengthen the rotor of the prototype machine by increasing the sleeve
17 thickness from 1mm to 3mm according to the design scheme proposed in the new Section V. We also
18 conduct the on-load experiment at the speed of 90krpm and the light load condition due to the limitation
19 of inverter capacity. Moreover, the thermal performances are also tested during the long time duration
20 experiment at the speed of 90krpm. The measured results indict the thermal equilibrium. The rotor also
21 runs well without any abnormalities, which verifies the validity of the proposed design scheme. In
22 addition, we add the details of the prototype machine fabrication process which is also very important
23 for the rotor mechanical robustness including the sleeve axial pressing, rotor balancing and bearing
24 selection. We reorganize and rewrite the experimental part (Section VI) in the revised manuscript. We
25 hope all these added results have improved the suitability of experimental results.
26
27
28
29
30
31

32 **3. Presentation issues**

33 Thank you for your comments. We redraw the figures according to the reviewers' suggestions. We also
34 do the proofreading with the help of a native English. All the typos and mistakes have been corrected.
35
36

37 Overall, all the revisions are highlighted in red and the corresponding point-by-point responses to the
38 reviewers' comments are enclosed as follows.
39
40
41
42

43 **Reviewer 1:**

44 Comments to the Author:

45 The paper presents rotor stress analysis of high speed surface mounted PM machines using carbon fiber
46 sleeves and segmented magnets. 2D FEA is used to identify the maximum tangential stress and the
47 contact pressure. Worst case scenarios are identified based on operating conditions. The organization of
48 the paper is clear, however, the method presented is not new, and how the experiments can validate the
49 design method is not clear. Please find some detailed points below:
50
51

- 52 (1) The prototype used in the experiment is running at much lower surface speed compared to the
53 design in Table I. It should be discussed why the prototype can validate the design method;
54

55 **Response:**

56 Thank you for your excellent comment. We take this issue very seriously. We are really sorry about
57 the weak experimental validation in the previous manuscript. In order to validate the rotor stability at a
58 higher speed. We strengthen the rotor of the prototype machine by increasing the sleeve thickness from
59 1mm to 3mm according to the design scheme proposed in the new Section V. We also conduct the on-
60

load experiment at the speed of 90krpm and the light load condition due to the limitation of inverter capacity. Moreover, the thermal performances are also tested during the long time duration experiment at the speed of 90krpm. The measured results indict the thermal equilibrium. The rotor also runs well without any abnormalities, which verifies the validity of the proposed design scheme. We hope all these added results have addressed your concern.

- (2) The black dashed line (PM tangential stress=0) is a bit misleading. It is recommend to re-arrange the axis labels and put 0 label next to this line.

Response:

Thank you for your comment. We redraw this figure and put 0 label next to the dashed line.

- (3) How the segmentation is modeled in 2D FEA is not clear (how large the slits are, how the nonlinearity at large displacement is modelled etc.).

Response:

Thank you for your excellent comment. In order to explain how the segmentation is modelled, we add the following in the revised manuscript: "The slits between segment magnets are set to be 0.1mm referred from [19]. The potential contact condition is set to be frictional which means the displacements in the circumferential direction are allowed."

Reviewer 2:

Comments to the Author:

In this paper, the rotor stress is analyzed for a 6-slot 4-pole high speed permanent magnet machine with segmented magnets retained by a carbon-fibre sleeve. The rotor PM segmentation is considered in the stress analysis of high-speed PM machines. The tangential stress of the PM and the sleeve, and the pressure between the segmented PMs are obtained. I have a few general questions and remarks.

- (1) P. 2, section I, left column, 2nd paragraph, line 6: ... it is essential to find the worst operating scenarios with respect to operating speed and temperature for each component of the rotor. In addition to checking the stress at the highest temperature and speed, how to find the worst operating scenarios.

Response:

Thank you for your comments. As can be seen from Fig.7, Fig.10 and Fig.11, the rotor stress monotonically increases or decreases with the temperature or speed. Hence, the worst operating scenarios must occur at the highest or lowest temperature or speed.

- (2) The author has done a lot of stress simulation, how to consider the influence of processing on the material properties.

Response:

Thank you for your comment. The reviewer is right. It is true the manufacturing process will have an impact on the rotor material especially the sleeves. We add the following in the manuscript: "The deterioration effect factor 2.5 due to manufacturing is considered in the allowable material limit. Hence, the tensile strength of carbon fiber sleeve is considered to be 1440MPa which is lower than the value in the data sheet of carbon fiber material."

On the other hand, the interference fit is also limited in real cases. "In addition, the maximum value

1
2
3 of interference fit is also limited by the sleeve outer diameter and CTE when the retaining sleeve is cold-
4 shrunk into the segmented PMs.”

- 5
6
7 (3) In Fig. 2, whether 3D is a simple 2D extension or 3D modeling. In the calculation conditions,
8 how to consider the connection of the end of the sheath, please give some details.

9
10 **Response:**

11 Thank you for your comment. The 3D modelling in this paper is the 2D extension. However, the axial
12 stress is considered in the 3D calculation. The potential axial stress is the main difference between the
13 2D and 3D FE calculations. For the investigated high speed PM machines, due to the low axial
14 length/diameter ratio, the results show that the axial stress is negligible.

- 15
16
17 (4) In Fig.7 (b), it is difficult to discern the influence of rotation speed and temperature on the
18 stress, please reconsider the drawing. Similarly, in Fig. 11, the author should consider rotating
19 the graph to more clearly reflect the influence of speed and temperature on the pressure between
20 the PMs. The current drawing is difficult to identify.

21
22 **Response:**

23 Thank you for your comment. We redraw those two figures in order to make it clear to identify.

- 24
25 (5) How to consider the gap between the segmented PMs, is there any filler? Missing the details
26 of this part, please add.

27
28 **Response:**

29 Thank you for your excellent comment. In order to explain how the segmentation is modelled, we
30 add the following in the revised manuscript: “The slits between segment magnets are set to be 0.1mm
31 referred from [19]. The potential contact condition is set to be frictional which means the displacements
32 in the circumferential direction are allowed.”

- 33
34
35 (6) In Fig. 14, Hb in the legend is not given in the text. In addition, the effect of Hb on the output
36 torque needs to be supplemented so that the content is more complete.

37
38 **Response:**

39 Thank you for your comment. We add the explanation of Hb in the text. In addition, the influence of
40 sleeve thickness on the output is also added in Section V: “However, the effective air gap length will be
41 inevitably increased due to the presence of retaining sleeve. The air gap flux density will thereby be
42 reduced, resulting in a lower output torque/torque density. Hence, the appropriate design of sleeve
43 thickness is quite important for both the mechanical and electromagnetic performance.”

- 44
45
46
47 (7) P. 5, In the experimental part, the author only gave the no-load back EMF and harmonic data
48 of 20,000 rpm. The electromagnetic error is 10%. Please analyze the source of this part of the
49 error. In addition, the details of the experiment should be added. The current speed is still far
50 from the rated speed of 100krpm, but the rotor strength test requires over-speed testing of the
51 motor to verify the reliability of the rotor machinery. Please supplement this part of the test
52 results as much as possible.

53
54
55 **Response:**

56
57 Thank you for your suggestion. We have identified the sources for the difference between the
58 measured and predicted results. We also add the details of the conducted experiment: “The prototype
59 machine is driven by the dynamometer shown in Fig. 18(b). The measured and simulated open-circuit
60

1
2
3 back-EMFs and corresponding spectra are shown in Fig.19 and Fig.20. Although there is a 10%
4 difference between the measured and predicted data, the good agreement can be observed. This
5 discrepancy can be attributed to the ignorance of end effect in the FE model. On the other hand, with
6 significant amount of the 5th and 7th harmonics, the back-EMF of the prototype machine is closer to a
7 trapezoidal waveform.”
8
9

10 In addition, we add the details of the prototype machine fabrication process which are also very
11 important for the rotor mechanical robustness including the sleeve axial pressing, rotor balancing and
12 bearing selection. In order to validate the rotor stability at a higher speed. We strengthen the rotor of the
13 prototype machine by increasing the sleeve thickness from 1mm to 3mm according to the design scheme
14 proposed in the adding Section V. We also conduct the on-load experiment at the speed of 90krpm and
15 the light load condition due to the limitation of inverter capacity. Moreover, the thermal performances
16 are also tested during the long time duration experiment at the speed of 90krpm. The measured results
17 indict the thermal equilibrium. The rotor also runs well without any abnormalities, which verifies the
18 validity of the proposed design scheme.
19
20
21
22
23
24
25

26 **Reviewer 3:**

27 Comments to the Author:

28 This paper analyses the rotor stress for a high-speed PM machine with segmented magnets retained by
29 carbon-fibre sleeve. There are several suggestions:

- 30
31 (1) The test experiments for verification is too simple for analysis.
32

33 **Response:**

34 Thank you for your comment. We are really sorry about the weak experimental validation in the
35 previous manuscript. We add the details of the conducted experiment: “The prototype machine is driven
36 by the dynamometer shown in Fig. 18(b). The measured and simulated open-circuit back-EMFs and
37 corresponding spectra are shown in Fig.19 and Fig.20. Although there is a 10% difference between the
38 measured and predicted data, the good agreement can be observed. This discrepancy can be attributed to
39 the ignorance of end effect in the FE model. On the other hand, with significant amount of the 5th and 7th
40 harmonics, the back-EMF of the prototype machine is closer to a trapezoidal waveform.”
41
42
43

44 In order to validate the rotor stability at a higher speed. We strengthen the rotor of the prototype
45 machine by increasing the sleeve thickness from 1mm to 3mm according to the design scheme proposed
46 in the new Section V. We also conduct the on-load experiment at the speed of 90krpm and the light load
47 condition due to the limitation of inverter capacity. Moreover, the thermal performances are also tested
48 during the long time duration experiment at the speed of 90krpm. The measured results indict the thermal
49 equilibrium. The rotor also runs well without any abnormalities which indirectly verifies the validity of
50 the proposed design scheme.
51
52
53

54 In addition, we add the details of the prototype machine fabrication process which are also very
55 important for the rotor mechanical robustness including the sleeve axial pressing, rotor balancing and
56 bearing selection as “As shown in Fig.17 (a), the permanent magnets are circumferentially segmented
57 into four pieces. The pole arc to pole pitch ratio is designed to be 1 so that the localized stress can be
58 avoided at the inter-pole position. In addition, the PM outer diameter is designed to be 37.9mm from the
59
60

1
2
3 electromagnetic point of view. According to the relationship between the minimum sleeve thickness and
4 the rotor outer diameter shown in Fig.16 (b), the sleeve thickness is finally chosen to be 3mm so that the
5 PM tangential stress is kept negative at the maximum operating speed and room temperature. The
6 retaining sleeve is made of the prefabricated carbon fiber as shown in Fig.17 (b). The sleeve is axially
7 pressed onto the rotor glued with segmented magnets as shown in Fig. 17 (c), so that the pre-contact stress
8 can be established between the sleeve and magnets. On the other hand, in order to achieve the
9 maximum operating speed, the hybrid deep groove ball bearings with rubber seal on both sides are
10 selected as shown in Fig.17 (d). Fig.17 (e) shows the stator assembly of the prototype machine. Fig.17
11 (f) shows the rotor assembly whose balancing was done by drilling holes in the copper ring at both sides
12 of the rotor.”

13
14
15
16
17
18 (2) The specifications for the prototype machine should be concluded.

19 **Response:**

20 Thank you for your suggestion. The specifications have been added in the revised manuscript.

21
22
23 (3) There are not enough innovativeness in this paper. There are simulations and tests for analysis
24 of the rotor stress, it is only measuring, without mechanism analysis or monitoring scheme.

25 **Response:**

26 Thank you for your comment. We add the following in the introduction part to make the novelty of
27 our work more clear: “The main contribution of the paper can be summarized from two aspects. First of
28 all, the phenomenon of stress concentration is firstly discovered in the retaining sleeve of high speed PM
29 machines with segmented permanent magnets. The specific conditions and influential factors (e.g.
30 number of segment, sleeve thickness...) are then identified. Hence, it can more clearly determine how to
31 mitigate this localized stress in the sleeve. More importantly, due to the significant impact of retaining
32 sleeve thickness on both the mechanical and electromagnetic performances, a new design scheme of
33 sleeve thickness of high speed PM machines with segmented magnets is proposed based on the findings
34 on the worst case scenarios. The relationship between the minimum sleeve thickness and the rotor outer
35 diameter is calculated which can save the time-consuming iteration processing time in the post-check of
36 traditional mechanical design.” In order to better explain this proposed new design scheme, we add a
37 separate section (**Section V**) to discuss how to calculate the minimum sleeve thickness. The proposed
38 scheme of sleeve design is quite important for the electromagnetic and mechanical design of high speed
39 PM machines. More importantly, compared with conventional design methods, it is more efficient and
40 provides more insight for investigating the coupled multi-physics mechanism in high speed PM
41 machines. With the help of the proposed scheme, the iterations can be eliminated in the traditional post-
42 check of mechanical design. In addition, the real optimal solution with higher torque density can be found
43 more efficiently in the electromagnetic design without worrying about its mechanical validity. We also
44 add the details of this part in the abstract and conclusion. We hope these two mentioned aspects have
45 addressed your concerns.

46
47
48
49
50
51
52
53
54
55 **Reviewer 4:**

56 Comments to the Author:

57 Stress Analysis of a High-Speed Permanent Magnet Machine Rotor with Segmented Magnets Retained
58 by Carbon-Fibre Sleeve is presented by structural analysis. Although the analysis seems interesting but
59
60

1
2
3 it is just numerical without required analytical or experimental verification. Authors should consider
4 below points in their revised manuscript:

- 5
6 (1) Effect of the segmentation and sleeve is just evaluated on the mechanical performance, it is not
7 enough while segmentation will affect partial demagnetization of PM segments, flux
8 weakening performance and It is required that such analysis is performed as well.

9
10 **Response:**

11 Thank you for your suggestion. We have added the analysis of demagnetization and flux weakening
12 capabilities of the investigated high speed PM machines with segmented magnets in the Appendix.

- 13
14
15 (2) For the experimental verification just BEMF test result is presented and it is claimed that” The
16 safe running of rotor validates the previous stress analysis.“ how you could evaluate rotor
17 stability and temperature rise by open circuit EMF test please explain?

18
19 **Response:**

20 Thank you for your comment. The reviewer is right. The open-circuit EMF cannot be treated as the
21 full proof of the rotor mechanical stability. Hence, in order to validate the rotor stability at a higher speed,
22 we strengthen the rotor of the prototype machine by increasing the sleeve thickness from 1mm to 3mm
23 according to the design scheme proposed in the new Section V. We also conduct the on-load experiment
24 at the speed of 90krpm and the light load condition due to the limitation of inverter capacity. Moreover,
25 the thermal performances are also tested during the long time duration experiment at the speed of 90krpm.
26 The measured results indict the thermal equilibrium. The rotor also runs well without any abnormalities,
27 which indirectly verifies the validity of the proposed design scheme. In addition, we add the details of
28 the prototype machine fabrication process which is also very important for the rotor mechanical
29 robustness including the sleeve axial pressing, rotor balancing and bearing selection. We reorganize and
30 rewrite the experimental part (Section VI) in the revised manuscript. We hope all these added results are
31 capable of verifying the validity of the theory.

- 32
33
34 (3) Since the main idea of the paper is mechanical stability of rotor, therefore the analysis results
35 should be evaluated by a test that confirm long time safe operation and mechanical stability of
36 machine at rated load.

37
38 **Response:**

39 Thank you for your comment. As requested, we conduct the on-load long time duration operation at
40 the speed of 90krpm. The thermal performances are also tested during the long-time experiment at the
41 speed of 90krpm. The measured results indict the thermal equilibrium. The rotor also runs well without
42 any abnormalities, which indirectly verifies the validity of the proposed design scheme. Due to the
43 limited capacity of the inverter, only the light load condition can be satisfied. However, as pointed out in
44 this paper, the worst case scenario occurs at the minimum temperature (Table IV), and hence, it also
45 makes sense to test the machine at the light or no load condition.

- 46
47
48 (4) Thermal analysis of machine is required.

49
50 **Response:**

51 Thank you for your comment. We have added the thermal analysis of the investigated high speed
52 PM machines in the Appendix.